

Supporting Information

Microporous metal-organic framework with naphthalene diimide groups for high methane storage

Yingxiang Ye,^{a,b} Rui-Biao Lin,^b Hui Cui,^b Ali Alsalmeh,^c Wei Zhou,^d Taner Yildirim,^d Zhangjing Zhang,^{*a} Shengchang Xiang,^a and Banglin Chen^{*b}

^a*Fujian Provincial Key Laboratory of Polymer Materials, College of Chemistry and Materials Science, Fujian Normal University, 32 Shangsan Road, Fuzhou 350007, PR China. E-mail: zzhang@ffnu.edu.cn*

^b*Department of Chemistry, University of Texas at San Antonio, One UTSA Circle, San Antonio, Texas 78249-0698, United States E-mail: banglin.chen@utsa.edu*

^c*Chemistry Department, College of Science, King Saud University, P O Box 2455, Riyadh 11451, Saudi Arabia*

^d*Center for Neutron Research, National Institute of Standards and Technology, Gaithersburg, Maryland 20899-6102, United States*

Materials and Measurements: All starting materials and reagents are commercially available and used without further purification. Powder X-ray diffraction (PXRD) was carried out with a PANalytical X'Pert³ powder diffractometer equipped with a Cu sealed tube ($\lambda = 1.54184 \text{ \AA}$) at 40 kV and 40 mA over the 2θ range of 4-30°. The simulated pattern was produced using the Mercury V1.4 program and single-crystal diffraction data. **FJU-101** was prepared according to our previously reported procedure.¹

Gas adsorption measurements: A Micromeritics ASAP 2020 surface area analyzer was used to measure N₂ sorption isotherms. To have a guest-free framework, the fresh as-synthesized sample was guest-exchanged with dry acetone at least 10 times, filtered and degassed at 373 K until the outgas rate was 5 $\mu\text{mHg min}^{-1}$ prior to measurements. A sample of 202 mg was used for the sorption measurements and was maintained at 77 K with liquid nitrogen. High-pressure methane (CH₄) and hydrogen (H₂) adsorption measurements were performed at the Center for Neutron Research, National Institute of Standards and Technology (NIST) using a computer-controlled Sieverts apparatus, detail of which can be found in a previous publication.²

Derivation of the isosteric heat of adsorption (Q_{st})

A virial type expression of the following form was used to fit the CH₄ (or H₂) total adsorption isotherm data at 270 K and 296 K (or 77 K, 160 K, and 296 K).

$$\ln p = \ln N + \frac{1}{T} \sum_{i=0}^m a_i N_i + \sum_{i=0}^n b_i N_i \quad (1)$$

Here, P is the pressure expressed in bar, N is the amount adsorbed in mmol/g, T is the temperature in K, a_i and b_i are virial coefficients, and m , n represents the number of coefficients required to adequately describe the isotherms. m and n were gradually increased until the contribution of extra added a and b coefficients was deemed to be statistically insignificant towards the overall fit, as determined using the average value of the squared deviations from the experimental values was minimized. The values of the virial coefficients a_0 through a_m were then used to calculate the isosteric heat of adsorption using the following expression.

$$Q_{st} = -R \sum_{i=0}^m a_i N_i \quad (2)$$

Here, Q_{st} is the coverage-dependent isosteric heat of adsorption and R is the universal gas constant of 8.3147 J K⁻¹ mol⁻¹.

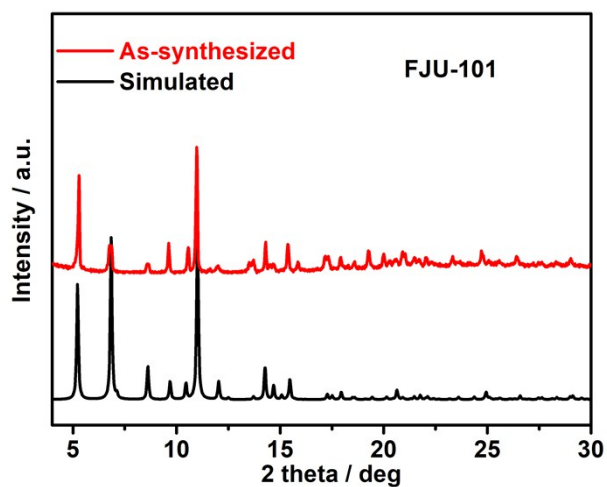


Figure S1. PXRD patterns of as-synthesized **FJU-101** (red) and the simulated XRD pattern from the single-crystal X-ray structure (black).

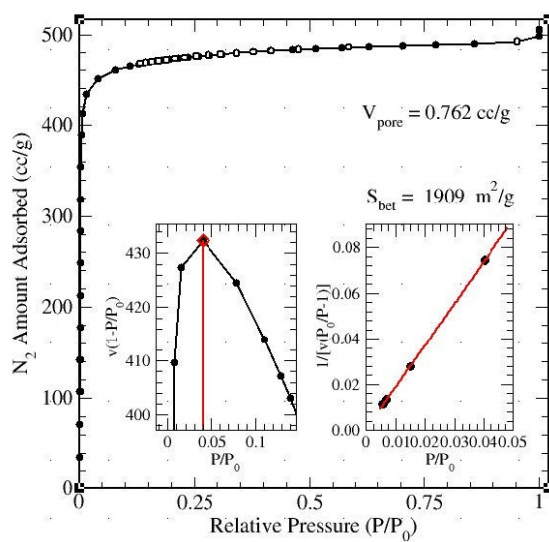


Figure S2. N_2 sorption isotherm of **FJU-101a** at 77 K. Solid and open symbols represent adsorption and desorption, respectively. Inset: BET plots for **FJU-101a**.

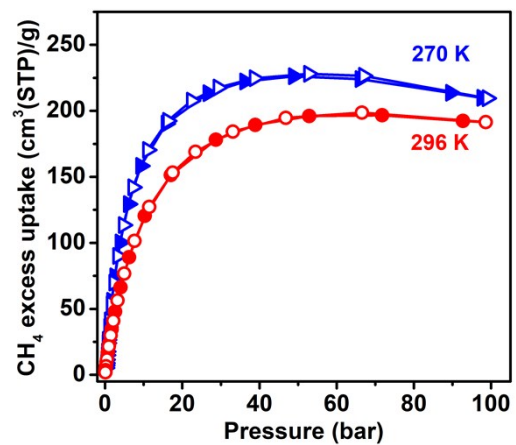


Figure S3. Excess high-pressure CH₄ adsorption isotherms of **FJU-101a** at 270 K and 296 K.

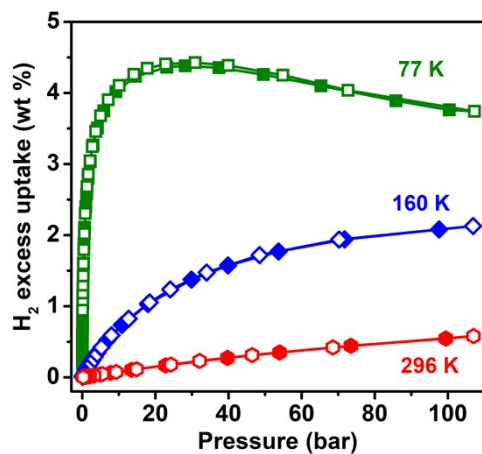


Figure S4. Excess high-pressure H₂ adsorption isotherms of **FJU-101a** at 77 K, 160 K and 296 K.

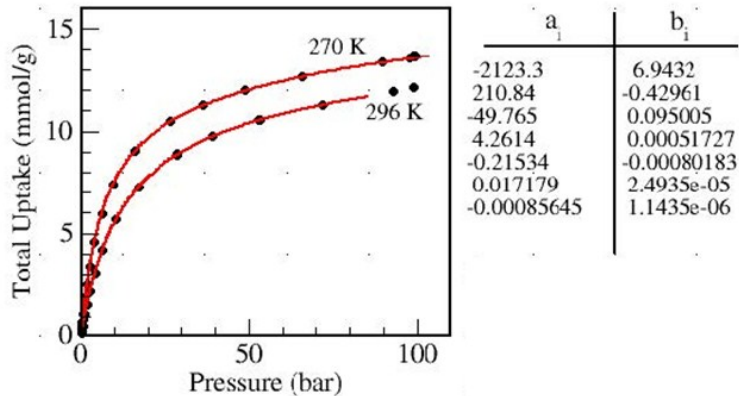


Figure S5. Derivation of Q_{st} for CH_4 adsorption in **FJU-101a** from virial fitting of the absolute adsorption isotherm data. The virial coefficients are shown on the right.

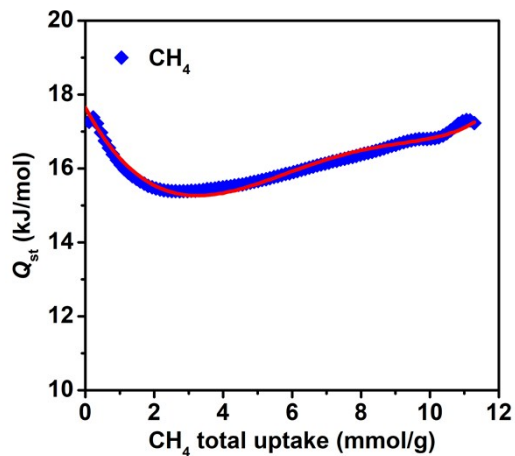


Figure S6. Isosteric heat of adsorption (Q_{st}) of CH_4 in **FJU-101a**, derived using the virial method.

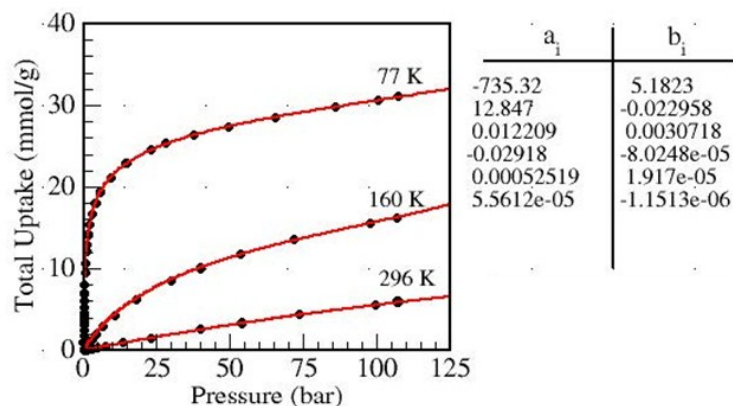


Figure S7. Derivation of Q_{st} for H_2 adsorption in **FJU-101a** from virial fitting of the absolute adsorption isotherm data. The virial coefficients are shown on the right.

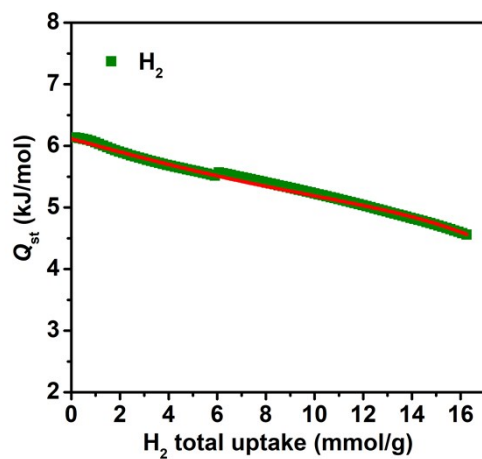


Figure S8. Isosteric heat of adsorption (Q_{st}) of H_2 in **FJU-101a**, derived using the virial method.

GCMC simulations

All the GCMC simulations were performed using the MS modeling 5.0 package.³ The framework and the individual methane molecule were considered to be rigid during the simulation. Partial charges for atoms of guest-free **FJU-101** were derived from QEq method and QEq_neutral1.0 parameter. Appropriate MOF supercells were chosen as the simulation boxes so that the dimensions are larger than $30 \times 30 \times 30 \text{ \AA}^3$. The simulation was carried out at 296 K, adopting the Fixed Loading task, Metropolis method in Sorption module and the universal force field (UFF). The partial charges on the atom of CH_4 (C: $-0.597e$, H: $0.149e$, where $e = 1.6022 \times 10^{-19} \text{ C}$ is the elementary charge) was also derived from QEq method. The interaction energy between methane molecule and framework was computed through the Coulomb and Lennard-Jones 6-12 (LJ) potentials. The cutoff radius was chosen as 15.5 \AA for the LJ potential and the long-range electrostatic interactions were handled using the Ewald & Group summation method. The loading steps and the equilibration steps were 1×10^6 , the production steps were 1×10^7 .

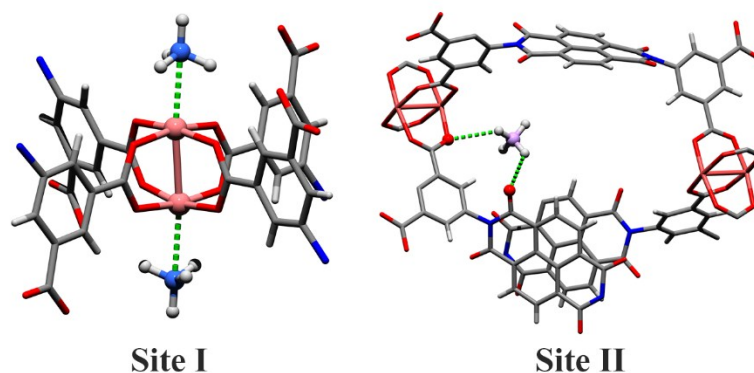


Figure S9. The primary (light blue) and secondary (lavender) CH_4 adsorption sites in **FJU-101a**, as revealed by GCMC simulation.

To understand the CH_4 adsorption mechanism, grand canonical Monte Carlo (GCMC) simulation was employed to investigate the interactions between **FJU-101a** and methane molecules. By performing a site-by-site search, two strong adsorption sites were found, at the open Cu sites and O sites, respectively (Fig. S9). The methane binding configuration at the open Cu site is consistent with CH_4 in the well-studied HKUST-1.⁴ The secondary CH_4 adsorption site is located at the corner of the quadrilateral window, where CH_4 can form hydrogen-bonding interactions with accessible carboxylate and naphthalene diimide groups. Thus, the high methane storage in **FJU-101a** is indeed attributed to potential functional sites (open metal and carbonyl group sites) and suitable pore cavities.

Disclaimer: Certain commercial equipment, instruments, or materials are identified in this paper to foster understanding. Such identification does not imply recommendation or endorsement by the National Institute of Standards and Technology, nor does it imply that the materials or equipment identified are necessarily the best available for the purpose.

Supplementary References

1. Y. Ye, Z. Ma, L. Chen, H. Lin, Q. Lin, L. Liu, Z. Li, S. Chen, Z. Zhang and S. Xiang, *J. Mater. Chem. A*, 2018, **6**, 20822-20828.
2. W. Zhou, H. Wu, M. R. Hartman and T. Yildirim, *J. Phys. Chem. C*, 2007, **111**, 16131-16137.
3. *Accelrys*, Materials Studio Getting Started, release 5.0, Accelrys Software, Inc., San Diego, CA, 2009.
4. H. Wu, J. M. Simmons, Y. Liu, C. M. Brown, X.-S. Wang, S. Ma, V. K. Peterson, P. D. Southon, C. J. Kepert, H.-C. Zhou, T. Yildirim and W. Zhou, *Chem. Eur. J.*, 2010, **16**, 5205-5214.